Robust Motion Correction Strategy for Structural MRI in Unsedated Children Demonstrated with Three-dimensional Radial MPnRAGE

Steven Kecskemeti, PhD • Alexey Samsonov, PhD • Julia Velikina, PhD • Aaron S. Field, MD, PhD • Patrick Turski, MD • Howard Rowley, MD • Janet E. Lainhart, MD • Andrew L. Alexander, PhD

From the Waisman Center (S.K., J.E.L., A.L.A.) and Departments of Radiology (S.K., A.S., A.S.F., P.T., H.R.), Medical Physics (J.V., A.L.A.), and Psychiatry (J.E.L., A.L.A.), University of Wisconsin–Madison, T123 Waisman Center, 1500 Highland Ave, Madison, WI 53705. Received January 22, 2018; revision requested March 20; final revision received June 4; accepted June 7. **Address correspondence to** S.K. (e-mail: *kecskemeti@wisc.edu*).

Supported by the National Institutes of Health Clinical Center (P50 MH100031, R01 MH097464, R21 EB018483, R21 HD078119, R21 NS091733, U01 AG051216) and the Waisman Center from the Eunice Kennedy Shriver National Institute of Child Health and Human Development (U54 HD090256).

Conflicts of interest are listed at the end of this article.

Radiology 2018; 289:509–516 • https://doi.org/10.1148/radiol.2018180180 • Content codes: MR PD

Purpose: To develop and evaluate a retrospective method to minimize motion artifacts in structural MRI.

Materials and Methods: The motion-correction strategy was developed for three-dimensional radial data collection and demonstrated with MPnRAGE, a technique that acquires high-resolution volumetric magnetization-prepared rapid gradient-echo, or MPRAGE, images with multiple tissue contrasts. Forty-four pediatric participants (32 with autism spectrum disorder [mean age ± standard deviation, 13 years ± 3] and 12 age-matched control participants [mean age, 12 years ± 3]) were imaged without sedation. Images with and images without retrospective motion correction were scored by using a Likert scale (0–4 for unusable to excellent) by two experienced neuroradiologists. The Tenengrad metric (a reference-free measure of image sharpness) and statistical analyses were performed to determine the effects of performing retrospective motion correction.

Results: MPnRAGE T1-weighted images with retrospective motion correction were all judged to have good or excellent quality. In some cases, retrospective motion correction improved the image quality from unusable (Likert score of 0) to good (Likert score of 3). Overall, motion correction improved mean Likert scores from 3.0 to 3.8 and reduced standard deviations from 1.1 to 0.4. Image quality was significantly improved with motion correction (Mann-Whitney *U* test; $P < .001$). Intraclass correlation coefficients for absolute agreement of Tenengrad scores with reviewers 1 and 2 were 0.92 and 0.88 ($P < .0005$ for both), respectively. In no cases did the retrospective motion correction induce severe image degradation.

Conclusion: Retrospective motion correction of MPnRAGE data were shown to be highly effective for consistently improving image quality of T1-weighted MRI in unsedated pediatric participants, while also enabling multiple tissue contrasts to be reconstructed for structural analysis.

Online supplemental material is available for this article.

MRI is inherently susceptible to motion. Faster and quieter imaging methods combined with behavioral strategies may enable imaging without sedation, but do not guarantee absence of motion artifacts (1,2). Many clinical imaging centers sedate children to reduce motion during imaging. However, the risk and adverse effects of sedation (2–5) prohibits the use in neuroimaging research.

Motion correction methods can improve MRI in uncooperative patients. In prospective methods, the imaging prescription is automatically adjusted to follow the object according to real-time motion estimates by using either optical tracking of target markers placed on the head (6) or continuously reacquired images from dedicated navigator scans (7). Both methods assume quiescent periods with minimal motion and reacquire data when this condition is not satisfied, which may result in even longer imaging times without substantial improvements to image quality. Additionally, optical tracking requires expensive hardware, needs a clear view of target markers, and may be sensitive to facial muscle movements.

Retrospective methods do not require expensive hardware, acquisition of dedicated navigators, or data reacquisition because they estimate motion and adjust the data as part of the image reconstruction process. One retrospective technique, periodically rotated overlapping parallel lines with enhanced reconstruction, or PROPELLER (8), has been clinically successful for in-plane (two-dimensional) (9,10) motion correction. However, correction of three-dimensional motion remains challenging because of limited efficiency of Cartesian sampling for three-dimensional self-navigation. One of the viable alternatives is radial sampling because it is more advantageous for data-based estimation of motion in three dimensions (11,12). Furthermore, motion effects are more benign in radial imaging, manifesting as blurring rather than as ghosting (13).

Three-dimensional radial sampling has other unique advantages for many clinical sequences (14–16). For example, combination of three-dimensional radials with magnetization-prepared rapid gradient echo (MPRAGE), one of the most common MRI methods in pediatric

Abbreviation

MPRAGE = magnetization-prepared rapid acquisition gradient echo

Summary

MPnRAGE with retrospective motion correction represents a robust imaging technique yielding consistently high-quality images with multiple T1-based contrasts in the presence of head motion.

Implication for Patient Care

Proposed retrospective motion correction may allow high-quality structural MRI in pediatric populations without the use of sedation.

neuroimaging (17), allowed generating multiple (*n* about 400) inversion-recovery contrast images in a single scan (a technique called MPnRAGE) (16). The purpose of our study was to develop and validate a retrospective method for motion-corrected multiple contrast structural imaging with MPnRAGE. We hypothesized that this method will significantly improve the success rate of structural MRI in pediatric participants without sedation. The motion correction was evaluated in cohorts of children with autism spectrum disorder and control participants.

Materials and Methods

Study Population

Imaging experiments were performed with institutional review board approval and informed consent or assent was obtained as part of a neuroimaging study of autism spectrum disorder from July 2014 to March 2016. MPnRAGE data were collected from 32 children with a diagnosis of autism spectrum disorder (mean age ± standard deviation, 155 months ± 36; range, 60–214 months) and 12 control participants (mean age, 142 months ± 32; range, 69–189 months). In total, 37 (28 with autism spectrum disorder) boys and seven (four with autism spectrum disorder) girls were included. Recruitment was not based on the likelihood of participants remaining still during imaging.

MPnRAGE Acquisition

MPnRAGE was implemented with a Discovery MR750 imager (General Electric Healthcare, Waukesha, Wis) with an inversion-recovery magnetization preparation and three-dimensional radial *k*-space acquisition (16). All participants watched a video of their choice during imaging and were instructed to remain still. Whole-brain MPnRAGE images were acquired sagittally at an isotropic resolution of 1.0 mm without parallel imaging. Parameters included delay time of 250 msec, repetition time of 4.6 msec, echo time of 1.7 msec, and *n* of 438 along the recovery curve. The excitation flip angles were 4°/6° for the first 326/remaining 112 views. The imaging time (approximately 8.5 minutes) was comparable with that of identically prescribed nonaccelerated MPRAGE (approximately 8 minutes).

MPnRAGE Motion Correction

Figure 1 illustrates the proposed motion-correction method as applied to MPnRAGE. The principal idea is to utilize subsets of consecutive *k*-space views acquired over a short duration to form a series of low-resolution three-dimensional navigator images for motion estimation via image-based registration techniques (18,19). The *k*-space data are then corrected by using these estimates before reconstruction of final full-resolution motion-corrected images.

The rate of motion tracking is determined by the number of views per navigator image. In our implementation, we exploit the MPnRAGE acquisition strategy to obtain navigators from the subsets of views between consecutive magnetization-preparation pulses (approximately 400 views every 2 seconds). The view ordering is performed by using double bit–reversed scheduling to maintain pseudorandom sampling both for all views between consecutive magnetization-preparation pulses and for each given view across multiple magnetization-preparation pulses (Fig 1). The first condition ensures full sampling in the central *k*-space for low-resolution navigator reconstruction. The second condition is necessary to obtain multiple-contrast images as described in references 16 and 20.

In our implementation, navigators are reconstructed at low resolution by apodizing the subsets of radial views with a Fermi filter. Motion parameters are estimated by using FSL library tools (*https://fsl.fmrib.ox.ac.uk/fsl/fslwiki*) for image coregistration (18,19). Finally, translational and rotational motion estimates are applied to the *k*-space data before final reconstruction (11).

Optimization of Navigator Resolution

Navigators reconstructed at suboptimal resolution may adversely affect motion estimates (eg, very low resolution may diminish the estimation of subtle motion, whereas too high resolution may introduce aliasing). Therefore, we evaluated motion correction for a range of navigator resolutions (2–10 mm) in four data sets with different motion characteristics (two with minimal, one with drift, and one with frequent arbitrary motions). Quality of motion correction versus navigator resolution was assessed by using the Tenengrad metric, a reference-free measure of image sharpness (21) agreeing well with human visual perception of natural images (20–22). The choice was motivated by the fact that the dominant effect of motion on radial imaging is blurring.

Image Quality Assessment

One midaxial, one off-center sagittal, and two coronal sections from both noncorrected and motion-corrected data sets were presented for scoring. Images were assessed independently by two blinded neuroradiologists (A.S.F. and P.T., with 17 and 36 years of experience, respectively) using a five-point Likert scale, as follows: 0, unusable (not acceptable for clinical use); 1, poor (minimal diagnostic use, reduced spatial resolution preventing distinction of white matter/gray matter boundaries across at least 50% of the observed brain, but large white matter structures still identifiable); 2, acceptable (white matter/gray matter generally identifiable but a significant loss of resolution and/or image artifacts has occurred that prevent clear white matter/gray matter boundaries); 3, good (well-defined white matter/gray matter boundaries over at least 50% of the brain; good signal-to-noise ratio and contrast-to-noise ratio; and few,

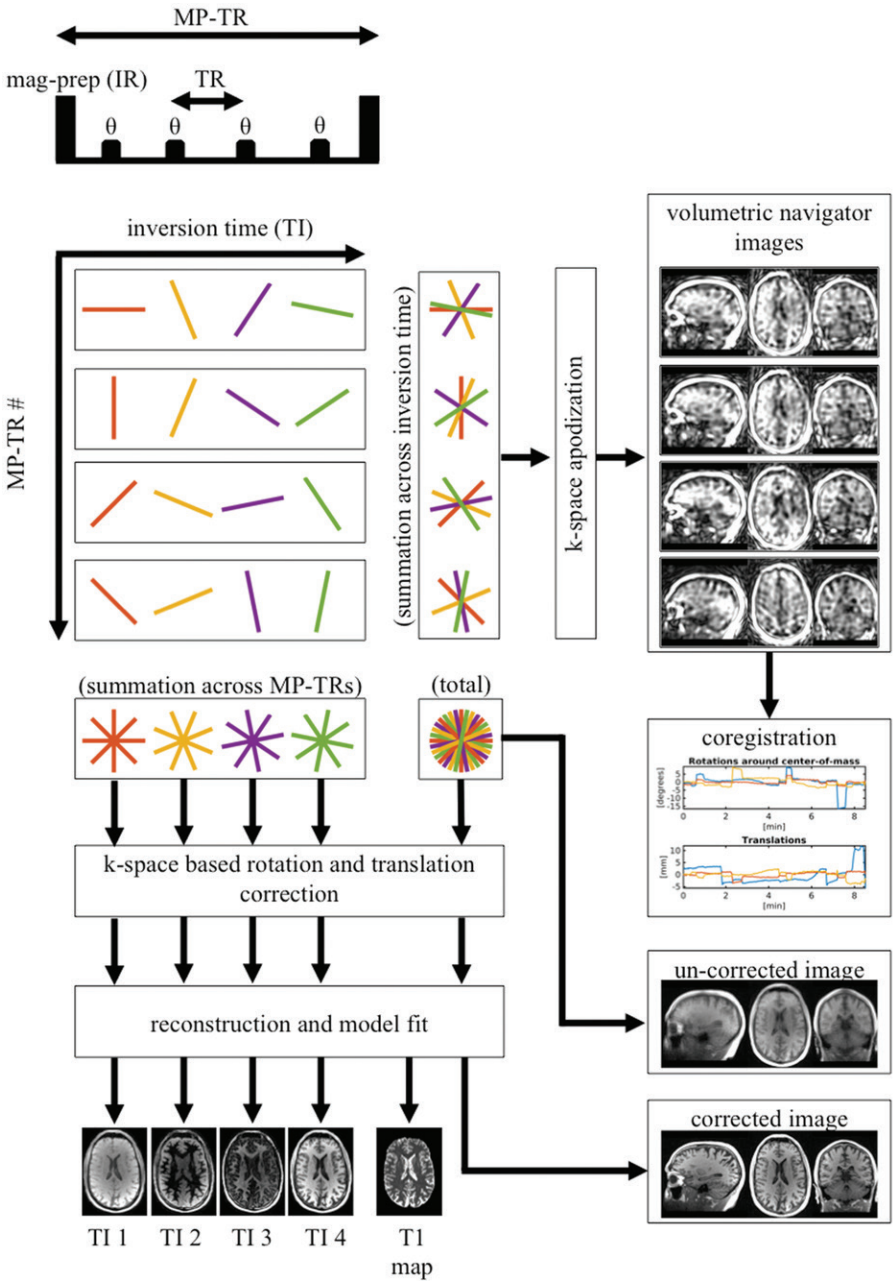

Figure 1: Schematic depicts motion-correction algorithm. For illustrative purposes, two-dimensional radial *k*-space sampling is depicted. Actual *k*-space sampling is three-dimensional radial. After each magnetic-preparation (MP) pulse, about 400 lines of *k*-space (over about 2 seconds) are sampled along inversion recovery curve (different effective inversion times). Views after each MP pulse form low-resolution navigator images, which are used to estimate translation and rotations between MP pulses via image-based registration. Raw *k*-space data are then corrected for translation and rotation before final image reconstruction is performed. TR = repetition time.

if any, artifacts); 4, excellent (well-defined white matter/gray matter boundaries across the entire brain, high signal-to-noise ratio and contrast-to-noise ratio, and no motion related artifacts present). The readers were allowed to choose a value of 3.5 (very good) when uncertain between 3 or 4. Motion-corrected and noncorrected image pairs for each participant were randomly counter-balance–ordered for presentation. Evaluators were allowed to toggle back and forth between the two sets of images to inspect them for subtle variations.

The automated image quality evaluation was performed by using the Tenengrad metric. The metric and percent change associated with motion correction were computed for each image pair and compared with the Likert ratings by using Pearson correlations.

Results

Optimization of Navigator Resolution

Figure 2 illustrates the effect of navigator resolution on motion correction. The maximum sharpness of motion-corrected images was attained for the 5–7-mm resolution range corresponding to up to 35% improvement over noncorrected images. In the studied navigator resolution range (2–10 mm), the sharpness of motion-corrected images deviated from its maximum value by 5%–11%, which signified moderate dependence of motion correction on the navigator resolution. The variability of image sharpness within the optimal navigator resolution range (5–7 mm) was minimal (<1%) for all data sets. The midrange value of 6 mm was selected for navigator resolution in the study.

Motion Characterization

Most frequent dominant motion types were translations in the superior-inferior direction and rotations of the sagittal plane. Table 1 summarizes the individual motion characteristics derived from the motion estimates.

Image Quality Evaluation

Table 2 and Figure 3 present results of radiologic evaluation. According to reviewer 1, motion correction improved the Likert scores from 1.0 to at least 3.5; no reduction of image quality after motion correction was detected. According to reviewer 2, motion correction improved the minimum Likert score from 0 to 3.0 (three cases); the slightly reduced scores of 3.5 were assigned to three out of the 14 cases scoring a maximum 4.0 before correction. Overall, the mean score increased from 3.0 to 3.8 and the standard deviation decreased from 1.1 to 0.4. A Mann-Whitney *U* test rejected the null hypothesis of equal medians before and after correction (reviewer 1, $z = -5.1$; $P < .001$; reviewer 2: $z = -4.0$; $P < .001$). Intraclass correlation coefficient (22) for the

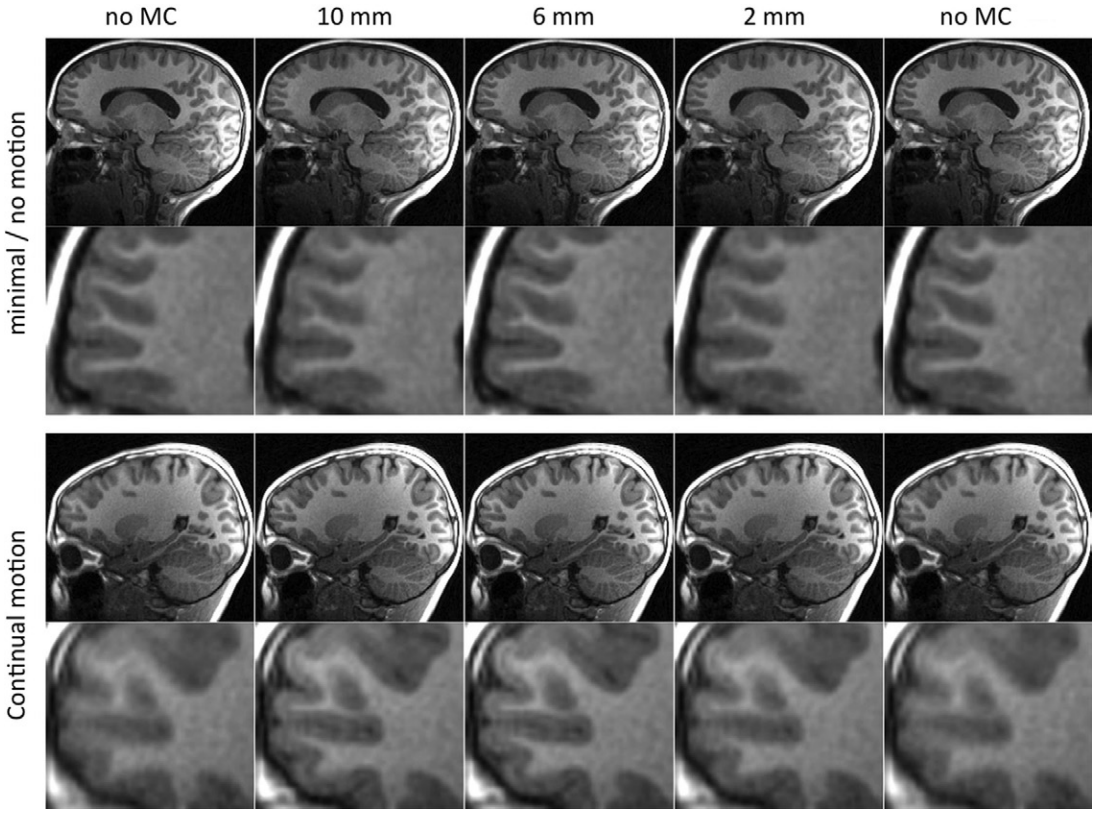

Figure 2: Comparison of images with no motion correction *(no MC)* and images with motion correction when different spatial resolutions were used for navigator images. Uncorrected images are displayed in both first and last columns to aid visualization and comparisons across columns. As distinctions in motion-corrected images that used navigator image resolutions between 4 mm and 7 mm could only be visualized with high zoom factors when display is toggled back and forth, only motion-corrected images formed by using lowest and highest resolution are shown, as well as final resolution used for this article.

degree of consistency between the raters was 0.90 ($P < .0005$) and 0.17 ($P = .13$) for noncorrected and corrected images, respectively, and intraclass correlation coefficient for absolute agreement for the change of scores because of motion correction was 0.88 ($P < .0005$).

Motion correction improved the Tenengrad image sharpness on average by 17% ± 28 (range, −5% to 103%). Figure 4 shows the percent changes in the Tenengrad metric against the reviewers' scores. The Pearson correlation coefficients of the percent changes in the Tenengrad metric versus the observers changes of Likert scores were 0.91 and 0.87 ($P < .0005$ for both) for reviewers 1 and 2, respectively.

Two cases for which the Likert score changed from 0 (unusable) to 3 (good) are illustrated in Figure 5 and Figure E1 (online). Figure 5 depicts a case of a 120-month-old boy with autism spectrum disorder with combination of continuous motion, 1–2-mm jitters, and rapid jump motion. The case of a 77-month-old girl with autism spectrum disorder (Fig E1 [online]) demonstrates motion correction for several 2–4-mm jumps followed

Table 1: Summary of Motion Transformations across All Participants

Parameter	Standard Deviation	Net
Translations in superior-inferior direction (mm)		
Autism spectrum disorder	0.7 (0.1, 2.7)	3.6 (0.8, 12.7)
Control participant	0.5 (0.1, 1.7)	3.0 (0.8, 11.0)
Total	0.6 (0.1, 2.7)	3.5 (0.8, 12.7)
Translations in left-right direction (mm)		
Autism spectrum disorder	0.2 (0.1, 0.6)	1.1 (0.4, 4.5)
Control participant	0.2 (0.1, 0.7)	1.3 (0.5, 5.8)
Total	0.2 (0.1, 0.7)	1.1 (0.4, 5.8)
Translations in anterior-posterior direction (mm)		
Autism spectrum disorder	0.2 (0.1, 0.8)	1.3 (0.5, 4.6)
Control participant	0.2 (0.1, 0.6)	1.8 (0.6, 6.4)
Total	0.2 (0.1, 0.8)	1.4 (0.5, 6.4)
Rotations of sagittal plane (degrees)		
Autism spectrum disorder	0.6 (0.2, 2.8)	4.1 (0.9, 18.9)
Control participant	0.6 (0.2, 2.3)	3.7 (1.3, 20.3)
Total	0.6 (0.2, 2.8)	4.0 (0.9, 20.3)
Rotations of coronal plane (degrees)		
Autism spectrum disorder	0.4 (0.2, 1.2)	2.2 (1.0, 6.6)
Control participant	0.4 (0.2, 0.8)	2.4 (1.0, 7.9)
Total	0.4 (0.2, 1.2)	2.3 (1.0, 7.9)
Rotations of axial plane (degrees)		
Autism spectrum disorder	0.4 (0.2, 2.2)	2.4 (0.8, 13.8)
Control participant	0.4 (0.2, 1.2)	2.7 (0.8, 9.4)
Total	0.4 (0.2, 2.2)	2.4 (0.8, 13.8)

Note.—Data in parentheses are minimum and maximum values.

Table 2: Effects on Likert Image Quality Scores after Performing Retrospective Motion Correction When Varying Amounts of Motion Are Present (44 Total Participants)

Likert Score before Motion Correction	No. of Participants before Motion Correction		After Motion Correction							
			Likert Score*		No. Decreased		No. Same		No. Increased	
	R1	R2	R1	R2	R1	R2	R1	R2	R1	R2
0	0	3	…	3 ± 0	0	0	0	0	0	3
1	4	4	3.9 ± 0.3	3 ± 0	0	0	0	0	4	4
2	6	7	4 ± 0	3.4 ± 0.4	0	0	0	0	6	7
3	7	9	4 ± 0	3.7 ± 0.4	0	0	0	2	7	7
3.5	9	7	3.8 ± 0.3	4 ± 0	0	0	3	0	6	7
4	18	14	4 ± 0	3.9 ± 0.2	0	3	18	11	0	0
0–4 (all)	44	44	3.2 ± 1.0	2.9 ± 1.2	0	3	21	13	23	28

Note.—Scores from two independent raters (reviewer 1 [*R1*] and reviewer 2 [*R2*]) are shown.
* Data are means ± standard deviations.

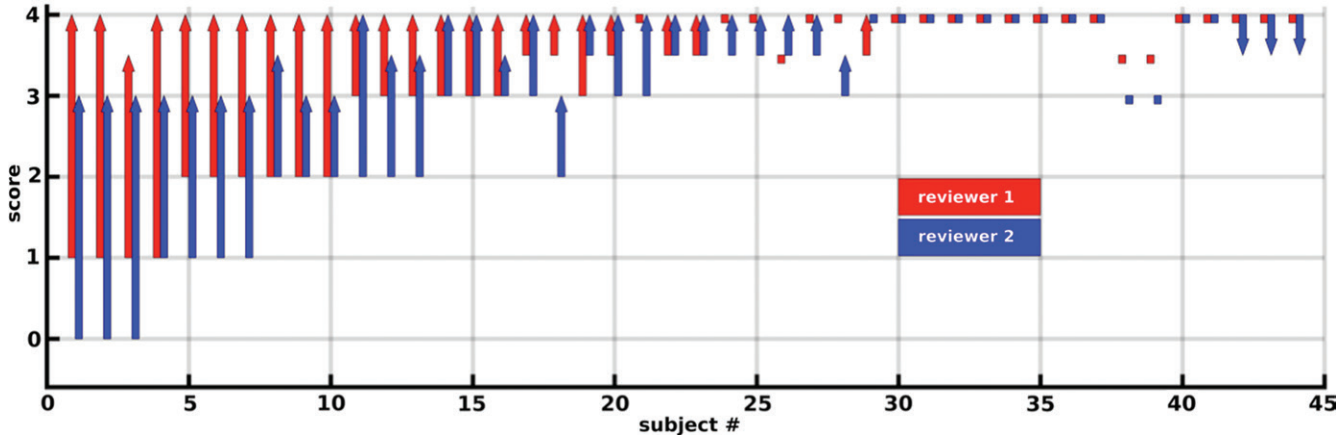

Figure 3: Graph shows Likert scores from radiologic assessment before (tail) and after (head) motion correction. For each participant, upward arrows indicate image quality improvement resulting from motion correction, whereas downward arrows indicate image quality degradation following motion correction.

by slow drifts. After motion correction, both white and gray matter are easily distinguished in both cases with well-defined boundaries. Figure E2 (online) shows effects of motion correction on multiple MPnRAGE contrasts. Figure 6 demonstrates the ability of the motion correction to reduce subtle blurring from small (approximately 0.4-mm) translations.

Discussion

We developed and evaluated a new retrospective motion-correction algorithm and demonstrated its utility for high-quality multicontrast structural T1-weighted MRI of nonsedated children in the presence of motion. The motion correction provided images of good to excellent quality, even when original images were poor or unusable. Subtle subvoxel motion was also corrected, improving delineation of white and gray matter boundaries.

It is critical for motion correction to maintain image quality when little to no motion is present, or to revert the changes if the applied processing results in loss of image quality. Our motion correction performed well for images that were originally highly scored (Likert score, 3.5–4). Specifically, over 80% (13 of 16) of cases originally scored 3.5 were improved to 4.0, whereas the rest retained the score. One reviewer reported slightly reduced scores (from 4.0 to 3.5) in three of 44 cases, whereas the other did not report any degradation. Importantly, our retrospective motion correction provides both corrected and noncorrected images, either of which can be presented for radiologic assessment. As our study revealed, the selection may be performed automatically by using the Tenengrad metric, which demonstrated high correspondence with radiologic evaluation. In contrast, prospective methods do not provide such an option because they yield only a single image, whose improvement is not guaranteed by motion correction (eg, in case of little to no motion).

Our current implementation targets motion occurring on the timescale of a single acquisition block (approximately 1.5–2.0 sec), which is comparable with timescales of other retrospective (8) and prospective (7) techniques. Correction at higher rates may be possible with development of dedicated methods for motion estimation within each navigator. Potential improvements

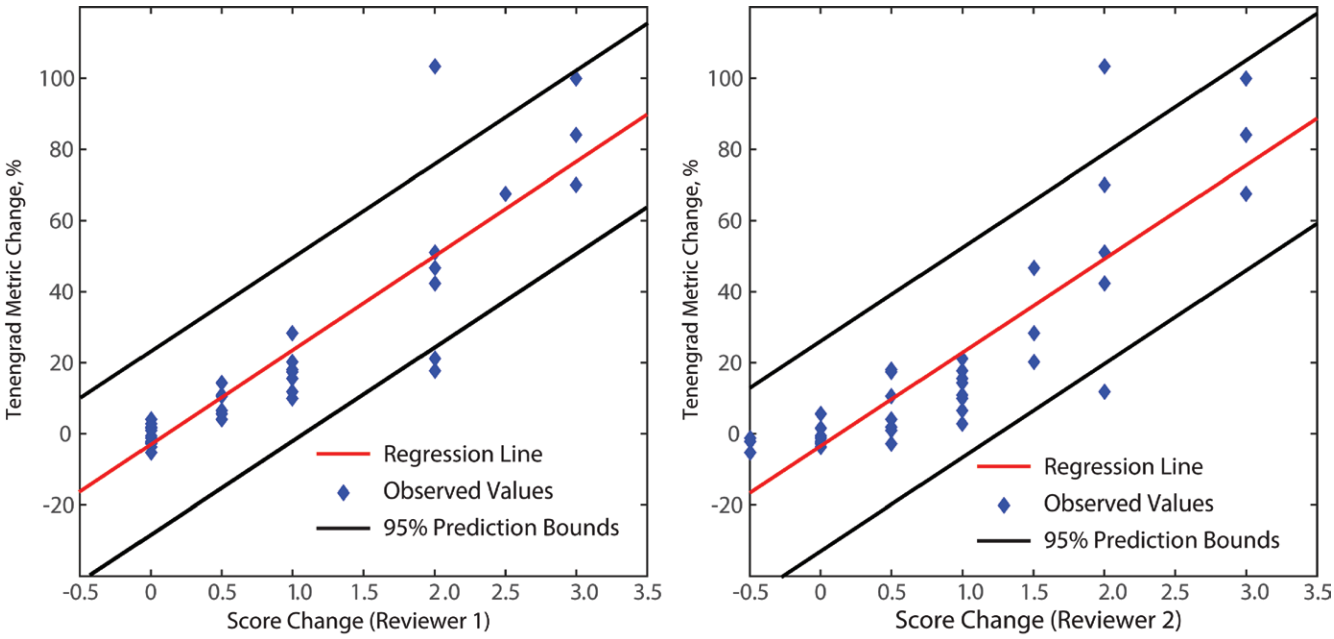

a. b.

Figure 4: Graphs show percent change of Tenengrad image sharpness measures before and after motion correction agree well with change in scores of image raters (Pearson correlation coefficients are 0.91 and 0.87; $P < .0005$ for both).

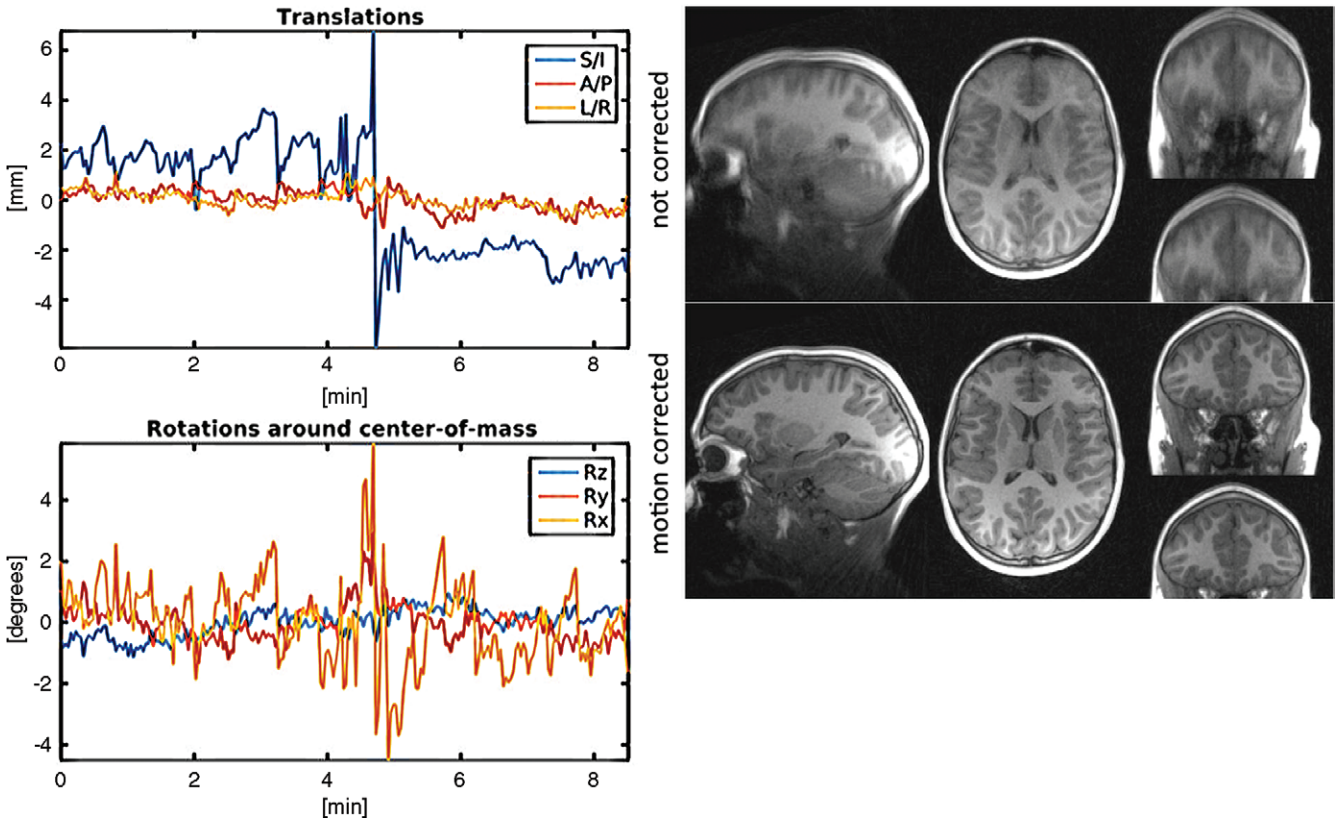

Figure 5: Reconstructed images in and motion estimates from a 120-month-old boy with autism spectrum disorder. Participant exhibited large amounts of nearly continuous motion in all three directions. Standard deviations of translations in superior-inferior, anterior-posterior, and right-left directions are 2.3 mm, 0.4 mm, and 0.4 mm, respectively. Standard deviations of rotations around *x (Rx), y (Ry),* and *z (Rz)* axes are 0.4°, 0.6°, and 1.4°, respectively. Radiologic scoring changed from 1 (poor) to 4 (excellent) for reviewer 1 and from 0 (not diagnostically useful) to 3 (good) for reviewer 2.

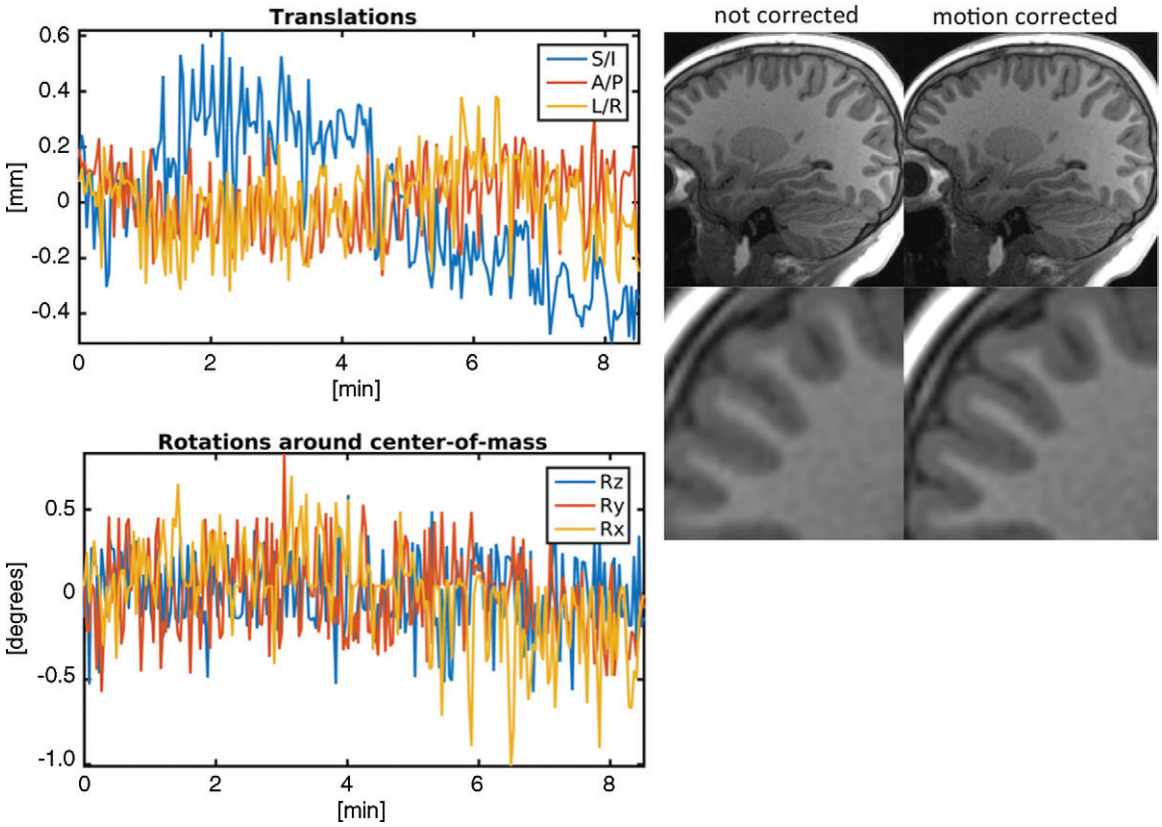

Figure 6: Reconstructed images in and motion estimates from a 172-month-old boy with autism spectrum disorder. Participant exhibited small sinusoidal motion in superior-inferior *(S/I)* direction with amplitude about 0.4 mm that produced slight blurring of white matter/gray matter and gray matter/cerebrospinal fluid boundaries that was only visible at high zoom factors. Retrospective motion correction reduced subtle blurring. *A/P* = anterior-posterior, *L/R* = left-right, *Rx* = *x* axis, *Ry* = *y* axis, *Rz* = *z* axis.

also include adaptive data weighting (23) or rejection (24) to deemphasize data acquired during periods of rapid motion or the use of parallel imaging and compressed sensing or low-rank reconstructions to reduce acquisition time and increase participant compliance. Our motion correction may be also combined with prospective motion navigators. Combining retrospective and prospective strategies was demonstrated to yield images of quality superior to the individual techniques (24). Additionally, our method can be applied to other sequences utilizing radial *k*-space acquisitions such as silent (25) and zero echo time, as well as other image contrasts (14,15).

In summary, MPnRAGE with retrospective motion correction represents a robust imaging technique yielding consistently high-quality images with multiple T1-based contrasts in the presence of head motion. Thus, this is a promising technique for generating high quality structural images in studies of children and individuals with intellectual impairment without sedation. Furthermore, although our study focused on pediatric MRI, motion correctable MPnRAGE will be equally effective for studies of adult patients.

Author contributions: Guarantors of integrity of entire study, S.K., J.E.L., A.L.A.; study concepts/study design or data acquisition or data analysis/interpretation, all authors; manuscript drafting or manuscript revision for important intellectual content, all authors; approval of final version of submitted manuscript, all authors; agrees to ensure any questions related to the work are appropriately resolved, all authors; literature research, S.K., A.S., J.V., A.L.A.; clinical studies, H.R., J.E.L.; experimental studies, S.K., A.S., J.V., P.T., H.R.; statistical analysis, S.K., A.S., J.V.; and manuscript editing, S.K., A.S., J.V., A.S.F., P.T., H.R., A.L.A.

Disclosures of Conflicts of Interest: S.K. Activities related to the present article: disclosed no relevant relationships. Activities not related to the present article: received payment for patent from institution. Other relationships: disclosed no relevant relationships. **A.S.** disclosed no relevant relationships. **J.V.** disclosed no relevant relationships. **A.S.F.** disclosed no relevant relationships. **P.T.** disclosed no relevant relationships. **H.R.** Activities related to the present article: disclosed no relevant relationships. Activities not related to the present article: disclosed no relevant relationships. Other relationships: received payment for patent disclosure from Wisconsin Alumni Research Foundation. **J.E.L.** disclosed no relevant relationships. **A.L.A.** Activities related to the present article: disclosed no relevant relationships. Activities not related to the present article: is member of external advisory board of Human Connectome Lifespan Project; is co-owner and scientific advisor of Thervoyant; received payment for expert testimony; received payment for grants/grants pending; is journal editor of *Neuroimage.* Other relationships: has patents/patents pending.

References

1. Nordahl CW, Mello M, Shen AM, et al. Methods for acquiring MRI data in children with autism spectrum disorder and intellectual impairment without the use of sedation. J Neurodev Disord 2016;8(1):20.
2. Rappaport BA, Suresh S, Hertz S, Evers AS, Orser BA. Anesthetic neurotoxicity: clinical implications of animal models. N Engl J Med 2015;372(9):796–797.
3. Bjur KA, Payne ET, Nemergut ME, Hu D, Flick RP. Anesthetic-related neurotoxicity and neuroimaging in children: a call for conversation. J Child Neurol 2017;32(6):594–602.
4. Lin EP, Lee JR, Lee CS, Deng M, Loepke AW. Do anesthetics harm the developing human brain? An integrative analysis of animal and human studies. Neurotoxicol Teratol 2017;60:117–128.
5. Barton K, Nickerson JP, Higgins T, Williams RK. Pediatric anesthesia and neurotoxicity: what the radiologist needs to know. Pediatr Radiol 2018;48(1):31–36.
6. Zaitsev M, Dold C, Sakas G, Hennig J, Speck O. Magnetic resonance imaging of freely moving objects: prospective real-time motion correction using an external optical motion tracking system. Neuroimage 2006;31(3):1038–1050.

7. White N, Roddey C, Shankaranarayanan A, et al. PROMO: real-time prospective motion correction in MRI using image-based tracking. Magn Reson Med 2010;63(1):91–105.
8. Pipe JG. Motion correction with PROPELLER MRI: application to head motion and free-breathing cardiac imaging. Magn Reson Med 1999;42(5):963–969.
9. Vertinsky AT, Rubesova E, Krasnokutsky MV, et al. Performance of PROPELLER relative to standard FSE T2-weighted imaging in pediatric brain MRI. Pediatr Radiol 2009;39(10):1038–1047.
10. Forbes KP, Pipe JG, Karis JP, Farthing V, Heiserman JE. Brain imaging in the unsedated pediatric patient: comparison of periodically rotated overlapping parallel lines with enhanced reconstruction and single-shot fast spin-echo sequences. AJNR Am J Neuroradiol 2003;24(5):794–798.
11. Anderson AG 3rd, Velikina J, Block W, Wieben O, Samsonov A. Adaptive retrospective correction of motion artifacts in cranial MRI with multicoil three-dimensional radial acquisitions. Magn Reson Med 2013;69(4):1094–1103.
12. Feng L, Axel L, Chandarana H, Block KT, Sodickson DK, Otazo R. XD-GRASP: golden-angle radial MRI with reconstruction of extra motion-state dimensions using compressed sensing. Magn Reson Med 2016;75(2):775–788.
13. Glover GH, Pauly JM. Projection reconstruction techniques for reduction of motion effects in MRI. Magn Reson Med 1992;28(2):275–289.
14. Gu T, Korosec FR, Block WF, et al. PC VIPR: a high-speed 3D phase-contrast method for flow quantification and high-resolution angiography. AJNR Am J Neuroradiol 2005;26(4):743–749.
15. Johnson KM, Block WF, Reeder SB, Samsonov A. Improved least squares MR image reconstruction using estimates of k-space data consistency. Magn Reson Med 2012;67(6):1600–1608.
16. Kecskemeti S, Samsonov A, Hurley SA, Dean DC, Field A, Alexander AL. MPnRAGE: a technique to simultaneously acquire hundreds of differently contrasted MPRAGE images with applications to quantitative T1 mapping. Magn Reson Med 2016;75(3):1040–1053.
17. Mugler JP 3rd, Brookeman JR. Three-dimensional magnetization-prepared rapid gradient-echo imaging (3D MP RAGE). Magn Reson Med 1990;15(1):152–157.
18. Jenkinson M, Bannister P, Brady M, Smith S. Improved optimization for the robust and accurate linear registration and motion correction of brain images. Neuroimage 2002;17(2):825–841.
19. Jenkinson M, Smith S. A global optimisation method for robust affine registration of brain images. Med Image Anal 2001;5(2):143–156.
20. Kecskemeti S, Johnson K, François CJ, Schiebler ML, Unal O. Volumetric late gadolinium-enhanced myocardial imaging with retrospective inversion time selection. J Magn Reson Imaging 2013;38(5):1276–1282.
21. Krotkov E. Focusing. Int J Comput Vis 1988;1(3):223–237.
22. McGraw KO, Wong SP. Forming inferences about some intraclass correlations coefficients. Psychol Methods 1996;1(1):30–46.
23. Roemer PB, Edelstein WA, Hayes CE, Souza SP, Mueller OM. The NMR phased array. Magn Reson Med 1990;16(2):192–225.
24. Samsonov AA, Velikina J, Jung Y, Kholmovski EG, Johnson CR, Block WF. POCS-enhanced correction of motion artifacts in parallel MRI. Magn Reson Med 2010;63(4):1104–1110.
25. Alibek S, Vogel M, Sun W, et al. Acoustic noise reduction in MRI using Silent Scan: an initial experience. Diagn Interv Radiol 2014;20(4):360–363.